Highly ordered *N*-heterocyclic carbene monolayers on Cu(111)

Eloise Angove[1], Federico Grillo[1], Herbert A Früchtl[1], Alex J. Veinot[2],

Ishwar Singh[2], J. Hugh Horton[2], Cathleen M Crudden[2,3], Christopher J Baddeley[1*]

1. EaStCHEM School of Chemistry, University of St Andrews, North Haugh, St Andrews, Fife, KY16 9ST
2. Department of Chemistry, Queen's University, 90 Bader Lane, Kingston, Ontario, Canada, K7L 3N6
3. Institute of Transformative Bio-Molecules, ITbM-WPI, Nagoya University, Nagoya, Chikusa 464-8601, Japan

* email cjb14@st-andrews.ac.uk

ABSTRACT: The benzannulated *N*-heterocyclic carbene, 1,3-dibenzylbenzimidazolylidene (NHC^{DBZ}) forms large, highly ordered domains when adsorbed on a Cu(111) surface under ultrahigh vacuum conditions. A combination of scanning tunnelling microscopy (STM), high resolution electron energy loss spectroscopy (HREELS) and density functional theory (DFT) calculations reveals that the overlayer consists of vertical benzannulated NHC moieties coordinating to Cu adatoms. Long range order results from the placement of the two benzyl units from a single NHC on opposite sides of the benzimidazole moiety, with the planes of their aromatic rings approximately parallel to the surface. The organization of three surface-bound benzyl substituents from three different NHCs into a triangular array controls the formation of a highly ordered Kagome-like lattice on the surface. This study illustrates the importance of dispersive interactions to control the binding geometry and self-assembly of the NHC.

N-heterocyclic carbenes (NHCs) are an emerging class of ligands for functionalizing extended metal surfaces, nanoparticles and nanoclusters.[1-16] The ability of NHCs to produce self-assembled monolayers on a range of metallic, non-metallic, and metalloid substrates has attracted considerable interest with potential applications in multiple fields including catalysis, microelectronics, biosensing, surface protection and 3D MOF architectures.[1,2,4,10, 14, 17-21] In such applications, it is critical to control the orientation and packing of NHC monolayers to fine-tune surface density, metal accessibility, and ligand orientation. Although the factors dictating binding orientation and self-assembly are not fully elucidated, several studies have pointed towards the important effect of wingtip substituents.[6,12, 14, 22-25] As summarized in Scheme 1 top, regardless of their backbone structures, NHCs with primary substituents including Me, Et, and Bu give ordered overlayers composed of flat-lying $M(NHC)_2$ species resulting from the abstraction of a metal atom (M) from the surface.[6, 12, 23-25] Bulky *N*-substituents such as ^{i}Pr, ^{t}Bu, Mes and 2,6-diIprAryl allow access to geometries whereby the heterocycle is perpendicular to the surface.[6, 12, 13, 14, 22-25] In the case of aryl substituents, van der Waals (vdW) interactions between the aromatic wingtips and the underlying gold surface were proposed to contribute significantly to the adsorption energy.[22] Recently, it was shown that NHCs with benzylic substituents can serve as initiation points for MOF formation from metal surfaces, but no information was provided on the organization or orientation of the NHC overlayers.[2]

In this work, we provide definitive evidence for the unique binding modes and surface structures obtainable from NHCs bearing flexible benzylic substituents. Cu(111) surfaces are employed because copper and its alloys have numerous applications in catalysis, microelectronics manufacturing and the production of wires, sheets and tubes. Scanning tunneling microscopy (STM), high resolution electron energy loss spectroscopy (HREELS) and density functional theory (DFT) calculations combine to demonstrate the formation of highly ordered, porous assemblies composed of entirely upright *N*-heterocycles. The aromatic rings adopt an approximately flat geometry providing additional stabilization via dispersive and weak covalent interactions [22]. Self-assembly of the benzene rings drives long range ordering into a Kagome-like lattice [26], (Scheme 1, bottom).
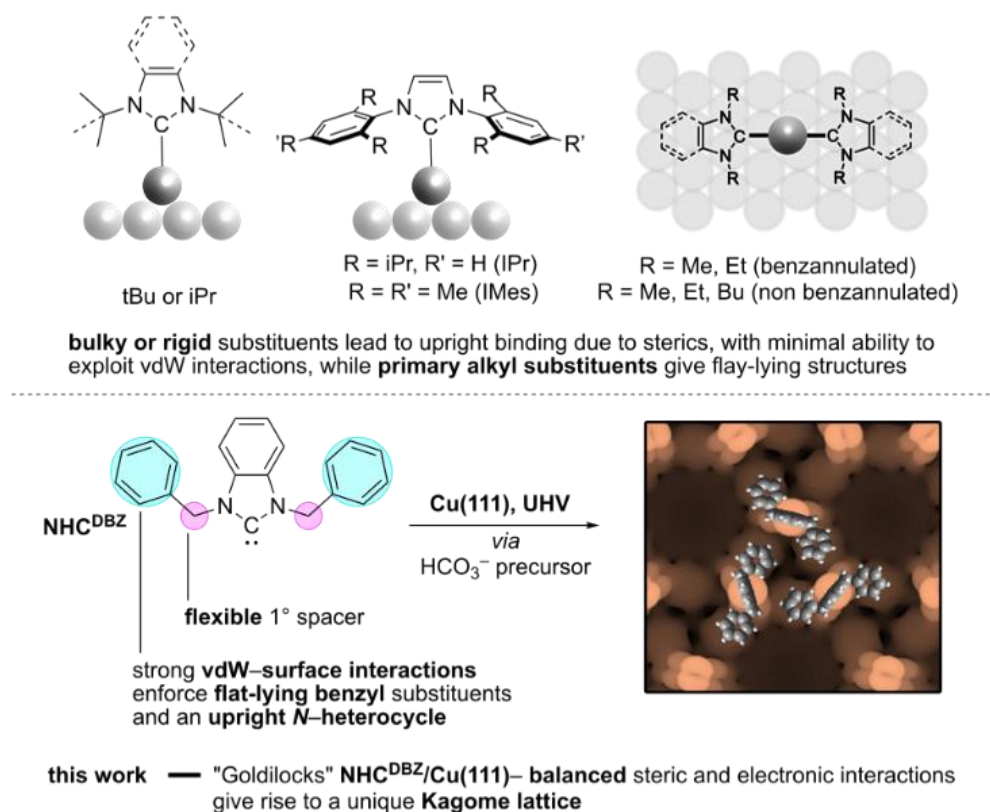
Scheme 1. Effects of benzylic wingtip groups on NHC adsorption geometry and assembly.

The hydrogen carbonate salt $NHC^{DBZ} \cdot H_2CO_3$ was prepared by simple benzylation of the parent benzimidazole and ion exchange (see Supporting Information, SI1). NHC overlayers were prepared by heating $NHC^{DBZ} \cdot H_2CO_3$ in a solid doser attached to the ultrahigh vacuum systems in direct line of sight to a Cu(111) sample. The resulting overlayers were examined by STM at room temperature. Small domains concentrated in the vicinity of step edges (figure 1a, arrows) appeared upon adsorption. Upon annealing to 430 K, the domain size of the observed overlayers increased dramatically, generating STM images as shown in figure 1b.
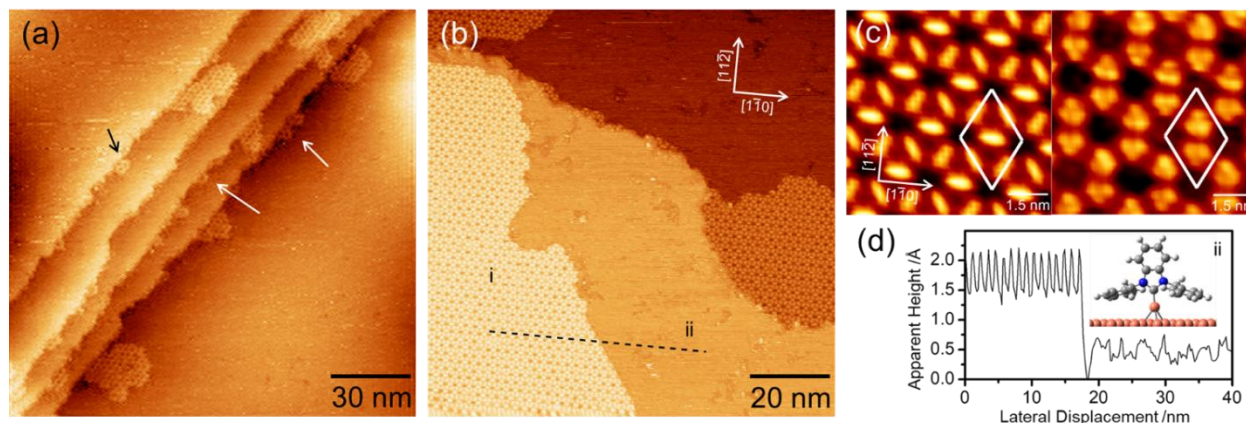
Figure 1. STM images acquired after dosing ~170 L (Langmuir) of NHC^{DBZ}/Cu(111) (a) as prepared, room temperature, 150×150 nm^2; (b) annealed to 430 K, 100×100 nm^2; (c) left, magnification of the "i" domain in (b), right, same domain recorded with different scanning parameters, both 7.5×7.5 nm^2; (d) line profile i in (b); all images -1.2 V, 0.25 nA, except (c, right) -1 V, 0.125 nA.

The ordered domains are characterized by a hexagonal arrangement of pores of diameter ~1 nm. Self-correlation analysis of several STM images reveals a unit cell dimension of 2.1 ± 0.1 nm along <1$\bar{1}$0> directions of the surface (white in figure 1c), consistent with the formation of a commensurate (8×8) overlayer (SI2). The higher contrast features that define the triangular units (figures 1c, left, -1.2 V bias) are assigned to the benzimidazole backbone. Under different imaging conditions (figure 1c, right, -1 V bias), three features whose shape and dimensions are consistent with the benzene rings of the NHC wingtips are observed within each triangular unit. This motif can only be generated if the two benzylic wingtip substituents take up a *trans* arrangement either side of an upright benzimidazolylidene unit,[27] which enables them to bridge two different triangular units. The propagation of adsorbates adopting this geometry generates the highly ordered porous domain structure. The cross-section ii in figure 1b (figure 1d) shows that at those specific scanning conditions, the molecular layer has an apparent height of ca. 1.5 Å, a value that cannot be taken as a true representation of the geometrical height. This clearly demonstrates that the STM contrast is dominated by electronic factors, as often observed for molecules adsorbed on metallic or semiconducting substrates.[28]

The ordered domains were found to be susceptible to some disruption whereby a domain present in one image would be perturbed by the STM tip in the next (SI3), especially for tunnelling currents >0.5 nA. This high mobility, coupled with the knowledge that the diffusion barrier for NHC species coordinated to gold adatoms has been computed to be about one order of magnitude lower than the diffusion barrier for NHC species bound to atoms in Au(111) terraces[17], suggests that the ordered domains consist of NHC^{DBZ} species coordinated to copper adatoms.

The incorporation of copper atoms in the self-assembly of other NHCs was reported by Larrea *et al*.[22] and has also been demonstrated following the adsorption of carboxylic acids and triazoles on copper surfaces[29-31]. Likely sources of copper atoms include low coordination sites at step edges and free copper adatoms which are present on low index copper surfaces[32]. The surface concentrations of adatoms on Cu(111) is known to be low [32], so extraction of copper atoms from step-edges is likely to drive the nucleation of molecular islands in the vicinity of steps. This is consistent with data shown in figure 1a, where initial overlayer formation occurs at step

edges. On annealing, islands accommodate further NHCs, and once sufficient thermal energy is available for surface diffusion, large islands propagate into the terrace.

On-surface DFT calculations (figure 2b) are in strong agreement with the STM images, leading to the conclusion that NHC^{DBZ} forms a commensurate (8×8) structure on Cu(111), with each NHC^{DBZ} attached to a copper adatom forming $Cu-NHC^{DBZ}$ species which self-assemble to produce ordered structures.
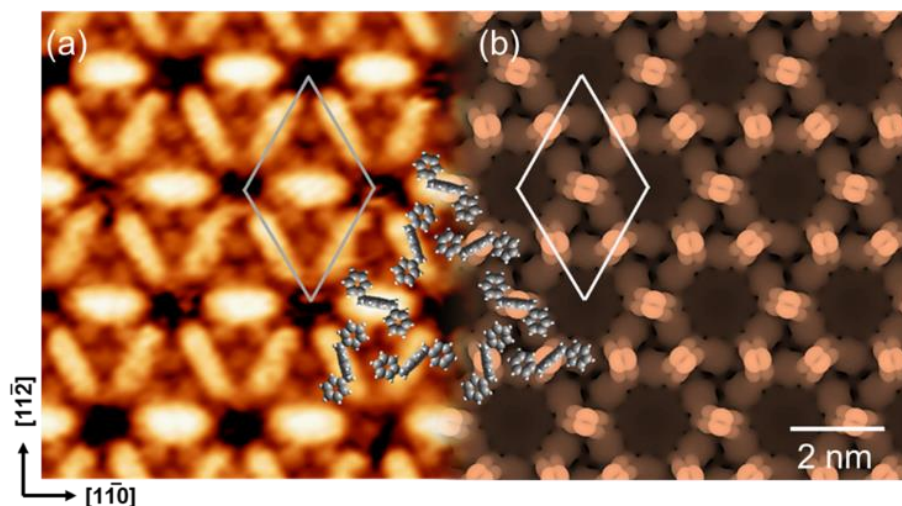

Figure 2. (a) STM topography of NHC^{DBZ}/Cu(111), thermal drift corrected, 10 × 10 nm^2, -1.2 V, 0.25 nA (b) simulated STM image at -1 V, of the (8×8) DFT model; between (a) and (b) superposed to scale molecular models; the unit cell is highlighted in both panels.

The overall molecular packing closely resembles a Kagome lattice. The relative position of the benzene rings is similar to the molecular separation in the $(\sqrt{7} \times \sqrt{7})R \pm 19.1°$ structure for benzene on Ni(111) [33] where neighboring adsorbates interleave to minimize repulsion between C-H groups.

Inconsistencies between the observed STM images and the DFT model presented in figure 2 deserve mention: pores observed in STM images (figure 2a) are smaller than those predicted by DFT modeling figure 2b, and the bright feature assigned to the benzimidazole backbone appears larger in the STM image than DFT calculations suggest. The large pore in the simulated STM image deviates from a perfect hexagonal structure. The most reasonable explanation for the observed images is that the benzimidazole unit and the copper atom to which it is coordinated slide backwards and forwards on the timescale of the STM image acquisition, giving rise to elongation of the bright features and shrinking of the pores.

No change in the periodicity of the ordered structure is observed following annealing across a wide temperature range, indicating that the Cu-NHC^{DBZ} complexes are thermally stable. TPD studies reported NHC desorption with a T_{max} of 550 K [21]. Desorption and surface decomposition processes compete such that disordered oligomeric species remain on the surface even after annealing to relatively high temperatures (SI4).

The tendency of NHC^{DBZ} to adsorb on Cu(111) with the benzimidazole moiety perpendicular to the surface contrasts to the behavior of *N,N*-dialkylbenzimidazolylidenes (R = Me, Et) and the simpler dimethylimidazolylidenes (R=Me, Et, Bu), all of which form flat-lying M(NHC)$_2$ complexes (Scheme 1, top) [6,12,23–25]. We compute that surface-bound *N,N*-dimethylbenzimidazolylidene is 0.45 eV more stable with the benzimidazole moiety parallel rather than perpendicular to the surface (SI5). In the case of NHC^{DBZ}, the energy cost associated with the benzimidazole moiety adopting a perpendicular geometry is more than compensated by the interaction of two aromatic *N*-substituents with the copper surface (SI5) considering that one molecule of benzene, in an optimized geometry, has an adsorption energy of ~0.8 eV on Cu(111).[34] Intermolecular interactions in the overlayer likely provide additional stabilization.

Further insight into the orientation of the NHC overlayers on Cu(111) was provided by HREELS (figure 3). Spectra were collected as a function of NHC^{DBZ} coverage and compared with the vibrational spectra of both *cis*- and *trans*-NHC^{DBZ} calculated via DFT. The main observed energy losses are attributed to an out-of-plane CH bend mode (γ_{CH}) of the phenyl/benzimidazole rings at 730 cm^{-1}, a twist of the -CH$_2$- at 1145 cm^{-1} (τ_{-CH2-}) and the aromatic CH stretch (ν_{CH}) at 3050 cm^{-1}. The latter peak shows a shoulder at ca. 2910 cm^{-1} due to the aliphatic ν_{CH} of the -CH$_2$-groups (SI6). A general increase in intensity of all bands is seen with increasing exposure (SI6). An adsorption geometry in which all aromatic rings were parallel to the surface would, by application of the metal surface dipole selection rule, yield a spectrum with an intense γ_{CH} mode at 730 cm^{-1} and a very weak ν_{CH} at 3050 cm^{-1}[23,31,35-37]. Instead, the γ_{CH}(730): ν_{CH}(3050) ratio indicates that one or more of the aromatic rings of NHC^{DBZ} is not parallel to the copper surface. This is consistent with STM results and unfavorable steric interactions in an "all planar" geometry (SI7).
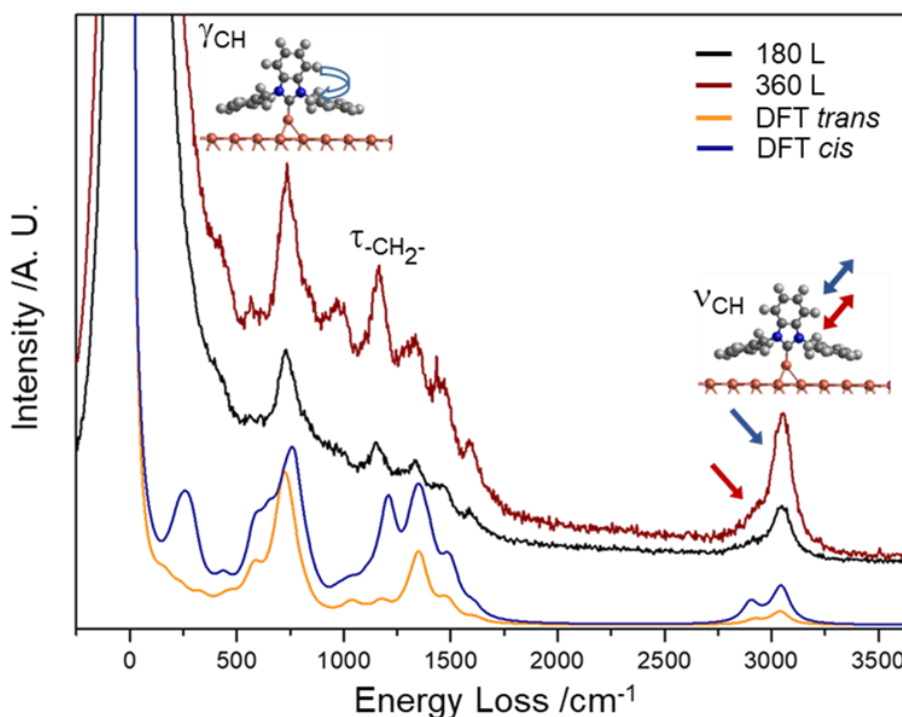
Figure 3. HREEL spectra collected following exposure of the Cu(111) sample to NHC^{DBZ} vapour at ~2×10^{-7} mbar and 300 K at increased coverage; black, 180 L; dark red, 360 L. In orange/blue the vibrational spectrum of *trans*/*cis* conformers calculated via DFT methods. Cartoons illustrate the main vibrations.

The simulated vibrational spectra of *trans*- and *cis*-NHCs bound to a copper atom are in close agreement with the experimental data and support the geometry proposed in light of the STM measurements. Simulations indicate that the fingerprints of both conformers contribute to the experimental spectra.

DFT was used to compare the adsorption energy of the two conformers of NHC^{DBZ} (SI8). For isolated adsorbates coordinated to copper adatoms, the *cis* species adsorbed with the heterocycle parallel to the surface was only ~0.14 eV more stable than the *trans* species adsorbed with the heterocycle upright. This suggests that *cis* NHC^{DBZ} may be present on the surface, but too mobile to image at 300 K. At higher temperatures, *cis* species can more readily overcome the activation barrier (calculated to be ~0.36 eV, SI9) to convert to *trans* species via rotation of the benzene rings around the -CH$_2$- group. This process would then augment the supply of *trans* species and allow for growth of ordered domains.

On the Cu(111) surface, *trans*-NHC[DBZ] can assume two enantiomeric configurations (Scheme 2). Since the surface is initially achiral, a racemic mixture of *trans*-Cu-NHC[DBZ] adsorbates exists over the whole surface. We were unable to identify which enantiomeric adsorption complex is present in each domain because the STM images have a higher symmetry than the model predicts, and we were unable to resolve features at domain edges which would help to distinguish enantiomers. If a mixture of enantiomers were present within a domain, one would predict many stacking faults within the molecular arrays or defects consisting of missing features. The lack of such defects suggests that the ordered domains are homochiral. (SI10)[38]
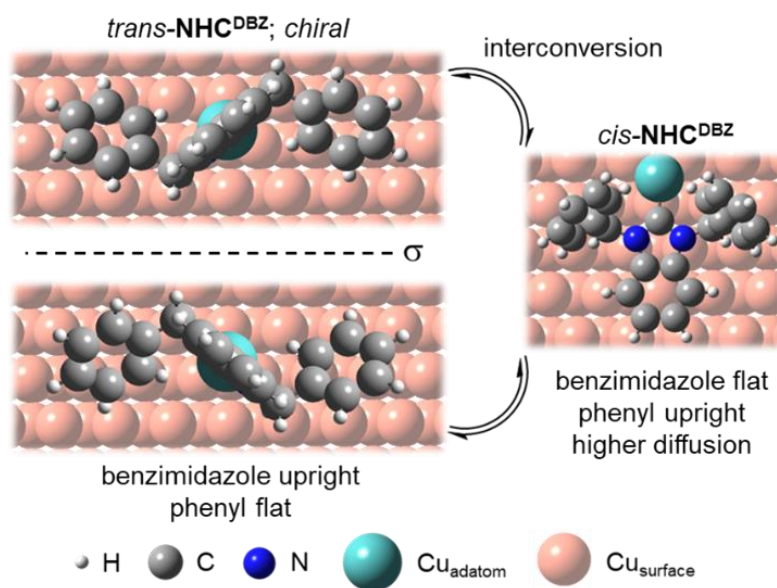
Scheme 2. Top views of NHC[DBZ] adsorption configurations on Cu(111), highlighting *trans/cis* interconversion and chirality of the *trans* conformer.

In this study, the adsorption behavior of NHC[DBZ] on Cu(111) was investigated. Cu-NHC[DBZ] species are formed on adsorption, presumably via extraction of copper atoms from step edges. Highly ordered and extended homochiral domains of Cu-NHC[DBZ] species are observed in STM images. DFT and STM reveal that the adsorbate forms ordered (8×8) arrays with three Cu-NHC[DBZ] species per unit cell. HREELS, DFT and STM show that the benzimidazole moiety adsorbs perpendicular to the surface with the phenyl rings of the benzylic substituents lying flat

and controlling the ordering of the overlayer into a Kagome-like lattice. These ordered overlayers generate well-defined nanosized pores, which are potentially of considerable utility in applications where confinement effects on this length scale are important. Moreover, when functionalised at the benzene end, the upright geometry of the benzimidazole opens the possibility to grow 3D structures.

ACKNOWLEDGMENT

REFERENCES

1   Godbold, P.; Johnson, G.; Obi, A. D.; Brown, R.; Hwang, S.; Robert J. Gilliard, J.; Zhang, S. Surfactant Removal for Colloidal Nanocrystal Catalysts Mediated by N-Heterocyclic Carbenes. *J. Am. Chem. Soc.* **2021**, *143*, 2644–2648.

2   Chang, L. M.; An, Y. Y.; Li, Q. H.; Gu, Z. G.; Han, Y. F.; Zhang, J. N-Heterocyclic Carbene as a Surface Platform for Assembly of Homochiral Metal-Organic Framework Thin Films in Chiral Sensing. *ACS Appl. Mater. Interfaces* **2020**, *12*, 38357–38364.

3   DeJesus, J. F.; Trujillo, M. J.; Camden, J. P.; Jenkins, D. M. N-Heterocyclic Carbenes as a Robust Platform for Surface-Enhanced Raman Spectroscopy. *J. Am. Chem. Soc.* **2018**, *140*, 1247–1250.

4   Zhukhovitskiy, A. V.; MacLeod, M. J.; Johnson, J. A. Carbene Ligands in Surface Chemistry: From Stabilization of Discrete Elemental Allotropes to Modification of Nanoscale and Bulk Substrates. *Chem. Rev.* **2015**, *115*, 11503–11532.

5   Engel, S.; Fritz, E.-C.; Ravoo, B. J. New Trends in the Functionalization of Metallic Gold: From Organosulfur Ligands to N-Heterocyclic Carbenes. *Chem. Soc. Rev.* **2017**, *46*, 2057–2075.

6   Inayeh, A.; Groome, R. R. K.; Singh, I.; Veinot, A. J.; de Lima, F. C.; Miwa, R. H.; Crudden, C. M.; McLean, A. B. Self-Assembly of N-Heterocyclic Carbenes on Au(111). *Nat. Commun.* **2021**, *12*, 1–9.

7   Yi, H.; Osten, K. M.; Levchenko, T. I.; Veinot, A. J.; Aramaki, Y.; Ooi, T.; Nambo, M.; Crudden, C. M. Synthesis and Enantioseparation of Chiral Au_{13} Nanoclusters Protected by Bis-N-Heterocyclic Carbene Ligands. *Chem. Sci.* **2021**, *12*, 10436–10440.

8   (a) Vignolle, J.; Tilley, T. D. N-Heterocyclic Carbene-Stabilized Gold Nanoparticles and Their Assembly into 3D Superlattices. *Chem. Commun.* **2009**, No. 46, 7230. (b) Hurst, E. C.; Wilson, K.; Fairlamb, I. J. S.; Chechik, V. N-Heterocyclic Carbene Coated Metal Nanoparticles. *New J. Chem.* **2009**, *33*, 1837.

9   Du, L.; Nosratabad, N. A.; Jin, Z.; Zhang, C.; Wang, S.; Chen, B.; Mattoussi, H. Luminescent Quantum Dots Stabilized by N-Heterocyclic Carbene Polymer Ligands. *J. Am. Chem. Soc.* **2021**, *143*, 1873–1884.

10   Smith, C. A.; Narouz, M. R.; Lummis, P. A.; Singh, I.; Nazemi, A.; Li, C. H.; Crudden, C. M. N-Heterocyclic Carbenes in Materials Chemistry. *Chemical Reviews.* **2019**, *119*, 4986–5056.

11   Crudden, C. M.; Horton, J. H.; Ebralidze, I. I.; Zenkina, O. V.; McLean, A. B.; Drevniok, B.; She, Z.; Kraatz, H.-B.; Mosey, N. J.; Seki, T.; Keske, E. C.; Leake, J. D.; Rousina-Webb, A.; Wu, G. Ultra Stable Self-Assembled Monolayers of N-Heterocyclic Carbenes on Gold. *Nat. Chem.* **2014**, *6*, 409–414.

12   Lovat, G.; Doud, E. A.; Lu, D.; Kladnik, G; Inkpen, M. S.; Steigerwald, M. L.; Cvetko, D.; Hybertsen, M. S.; Morgante, A.; Roy, X.; Venkataraman, L. Determination of the Structure and Geometry of N-Heterocyclic Carbenes on Au(111) Using High-Resolution Spectroscopy. *Chem. Sci.* **2019**, *10*, 930–935.

13   Wang, G.; Rühling, A.; Amirjalayer, S.; Knor, M.; Ernst, J. B.; Richter, C.; Gao, H.-J.; Timmer, A.; Gao, H.-Y.; Doltsinis, N. L.; Glorius, F.; Fuchs, H. Ballbot-Type Motion of N-Heterocyclic Carbenes on Gold Surfaces. *Nat. Chem.* **2017**, *9*, 152–156.

14   Zeng, Y.; Zhang, T.; Narouz, M. R.; Crudden, C. M.; McBreen, P. H. Generation and Conversion of an N-Heterocyclic Carbene on Pt(111). *Chem. Commun.* **2018**, *54*, 12527–12530.

15   Doud, E. A.; Starr, R. L.; Kladnik, G.; Voevodin, A.; Montes, E.; Arasu, N. P.; Zang, Y.; Zahl, P.; Morgante, A.; Venkataraman, L.; Vázquez, H.; Cvetko, D.; Roy, X. Cyclopropenylidenes as Strong Carbene Anchoring Groups on Au Surfaces. *J. Am. Chem. Soc.* **2020**, *142*, 19902–19906.

16   Knecht, P.; Zhang, B.; Reichert, J.; Duncan, D. A.; Schwarz, M.; Haag, F.; Ryan, P. T. P.; Lee, T.-L.; Deimel, P. S.; Feulner, P.; Allegretti, F.; Auwärter, W.; Médard, G.; Seitsonen, A. P.; Barth, J. V.; Papageorgiou, A. C. Assembly and Manipulation of a Prototypical N-Heterocyclic Carbene with a Metalloporphyrin Pedestal on a Solid Surface. *J. Am. Chem. Soc.* **2021**, *143*, 4433–4439.

17   Nguyen, D. T.; Freitag, M.; Körsgen, M.; Lamping, S.; Rühling, A.; Schäfer, A. H.; Siekman, M. H.; Arlinghaus, H. F.; van der Wiel, W. G.; Glorius, F.; Ravoo, B. J. Versatile Micropatterns of N-Heterocyclic Carbenes on Gold Surfaces: Increased Thermal and Pattern Stability with Enhanced Conductivity. *Angew. Chemie Int. Ed.* **2018**, *57*, 11465–11469.

18   She, Z.; Narouz, M. R.; Smith, C. A.; MacLean, A.; Loock, H.-P.; Kraatz, H.-B.; Crudden, C. M. N-Heterocyclic Carbene and Thiol Micropatterns Enable the Selective Deposition and Transfer of Copper Films. *Chem. Commun.* **2020**, *56*, 1275–1278.

19   Singh. I.; Lee, D. S.; Huang, S.; Bhattacharjee, H.; Xu, W.; McLeod, J. F.; Crudden, C. M.; She, Z. N-Heterocyclic Carbenes Meet Toll-like Receptors. *Chem. Commun.* **2021**, 57, 8421-8424.

20   Mayall, R. M.; Renaud-Young, M.; Gawron, E.; Luong, S.; Creager, S.; Birss, V. I. Ultrasensitive and Label-free Detection of the Measles Virus using an N-Heterocyclic Carbene-Based Electrochemical Biosensor. *ACS Sensors* **2020**, *5*, 2747–2752.

21   Crudden, C. M.; Horton, J. H.; Narouz, M. R.; Li, Z.; Smith, C. A.; Munro, K.; Baddeley, C. J.; Larrea, C. R.; Drevniok, B.; Thanabalasingam, B.; McLean, A. B.; Zenkina, O. V.; Ebralidze, I. I.; She, Z.; Kraatz, H. B.; Mosey, N. J.; Saunders, L. N.; Yagi, A. Simple Direct Formation of Self-Assembled N-Heterocyclic Carbene Monolayers on Gold and Their Application in Biosensing. *Nat. Commun.* **2016**, *7*, 12654.

22   Tang, Q.; Jiang, D.-E. Comprehensive View of the Ligand−Gold Interface from First Principles. *Chem. Mater* **2017**, *29*, 2021.

23   Larrea, C. R.; Baddeley, C. J.; Narouz, M. R.; Mosey, N. J.; Horton, J. H.; Crudden, C. M. *N* -Heterocyclic Carbene Self-Assembled Monolayers on Copper and Gold: Dramatic Effect of Wingtip Groups on Binding, Orientation and Assembly. *ChemPhysChem* **2017**, *18*, 3536–3539.

24   Jiang, L.; Zhang, B.; Paavo Seitsonen, A.; Haag, F.; Allegretti, F.; Reichert, J.; Kuster, B.; Barth, J. V; Papageorgiou, A. C. N-Heterocyclic Carbenes on Close-Packed Coinage Metal Surfaces: Bis-Carbene Metal Adatom Bonding Scheme of Monolayer Films on Au, Ag and Cu. *Chem. Sci.* **2017**, *8*, 8301–8308.

25   Bakker, A.; Timmer, A.; Kolodzeiski, E.; Freitag, M.; Gao, H. Y.; Mö, H.; Amirjalayer, S.; Glorius, F.; Fuchs, H. Elucidating the Binding Modes of N-Heterocyclic Carbenes on a Gold Surface. **2018**, 140, 11889-11892.

26   Mekata, M. Kagome: The Story of the Basketweave Lattice, *Phys. Today*, **2007**, 56, 12.

27   *cis*-NHC^{DBZ} is defined as the geometry where the benzyl units are on the same side of the benzimidazole moiety and *trans*-NHC^{DBZ} where the benzyl rings are on opposite sides.

28   Emsley, J. *Nature's building blocks: an A–Z guide to the elements*; Oxford University Press, 2003, pp 121–125.

29   Gattinoni, C.; Tsaousis, P.; Euaruksakul, C.; Price, R.; Duncan, D. A.; Pascal, T.; Prendergast, D.; Held, G.; Michaelides, A. Adsorption Behavior of Organic Molecules: A Study of Benzotriazole on Cu(111) with Spectroscopic and Theoretical Methods. *Langmuir* **2019**, *35*, 882–893.

30   Gattinoni, C.; Michaelides, A. Understanding Corrosion Inhibition with van Der Waals DFT Methods: The Case of Benzotriazole. *Faraday Discuss.* **2015**, *180*, 439–458.

31   Grillo, F.; Tee, D. W.; Francis, S. M.; Früchtl, H.; Richardson, N. V. Initial Stages of Benzotriazole Adsorption on the Cu(111) Surface. *Nanoscale Commun. Publ.* **2013**, *5*, 5269–5273.

32   Perry, C. C.; Haq, S.; Frederick, B. G.; Richardson, N. V. Face Specificity and the Role of Metal Adatoms in Molecular Reorientation at Surfaces. *Surf. Sci.* **1998**, *409*, 512–520.

33   Steinrück, H. P.; Huber, W.; Pache, T.; Menzel, D. The Adsorption of Benzene Mono- and Multilayers on Ni(111) Studied by TPD and LEED. *Surf. Sci.* **1989**, *218*, 293–316.

34   Lomas, J. R.; Baddeley, C. J.; Tikhov, M. S.; Lambert, R. M. Ethyne Cyclization to Benzene over Cu(110), *Langmuir*, **1995**, *11*, 3048-3053.

35   Grillo, F.; Tee, D. W.; Francis, S. M.; Früchtl, H. A.; Richardson, N. V. Passivation of Copper: Benzotriazole Films on Cu(111). *J. Phys. Chem. C* **2014**, *118*, 8667–8675.

36   Grillo, F.; Garrido Torres, J. A.; Treanor, M.-J.; Larrea, C. R.; Götze, J. P.; Lacovig, P.; Früchtl, H. A.; Schaub, R.; Richardson, N. V. Two-Dimensional Self-Assembly of Benzotriazole on an Inert Substrate. *Nanoscale* **2016**, *8*, 9167–9177.

37   Grillo, F.; Batchelor, D.; Larrea, C. R.; Francis, S. M.; Lacovig, P.; Richardson, N. V. On-surface condensation of low-dimensional benzotriazole-copper assemblies, *Nanoscale* **2019**, *11*, 13017-13031.

38   The computational model in Figure 2(b) shows a homochiral domain, but additional low temperature STM measurements would be required to address the issue of absolute chirality.